Effect of buoyancy forces on the flow and heat transfer over a continuous moving vertical or inclined surface

Ali J. Chamkha [a], Harmindar S. Takhar [b*], Girishwar Nath [c]

[a] *Mechanical and Industrial Engineering Department, Kuwait University, Safat 13060, Kuwait*
[b] *Department of Engineering and Technology, Manchester Metropolitan University, Manchester, M1 5GD, UK*
[c] *Department of Mathematics, Indian Institute of Science, Bangalore-560012, India*

Abstract — An analysis is performed to study the effect of the buoyancy forces on the flow and heat transfer over a heated vertical or inclined surface which moves with non-uniform velocity in an ambient fluid. Both the constant wall and constant heat flux conditions are considered. The coupled non-linear partial differential equations governing the flow are solved using an implicit finite-difference scheme. It is found that, beyond a certain value of the buoyancy parameter, the skin friction vanishes at certain locations, but it does not imply separation since we are considering the flow over a moving surface. Also for large buoyancy parameter, the velocity of the fluid near the wall exceeds that on the wall. The Nusselt number increases with the buoyancy parameter, the Prandtl number and the stream-wise distance. The Nusselt number for the constant heat flux case is found to be higher than that of the constant wall temperature case. © 2001 Éditions scientifiques et médicales Elsevier SAS

buoyancy effects / flow / heat transfer / inclined surfaces

Nomenclature

a	constant	
C_f	coefficient of skin friction	
g	acceleration due to gravity	$\mathrm{m \cdot s^{-2}}$
Gr	Grashoff number	
k	thermal conductivity	$\mathrm{W \cdot m^{-2} \cdot K^{-1}}$
L	chracteristic length	m
Pr	Prandtl number	
Re	Reynolds number	
q	rate of heat transfer	$\mathrm{W \cdot m^{-2}}$
R	denotes a dependent variable	
T	temperature	K
U	wall velocity	$\mathrm{m \cdot s^{-1}}$
u, v	velocity components	$\mathrm{m \cdot s^{-1}}$
x, y	Cartesian coordinates	

Greek symbols

α	thermal diffusivity	$\mathrm{m^2 \cdot s^{-1}}$
β	coefficient of thermal coefficient	
θ	dimensionless temperature	

ν	kinematic viscosity	$\mathrm{m^2 \cdot s^{-1}}$
ξ, η	similarity variables	
ϕ	angle of inclination of the surface	
Ψ	stream function	

Subscripts

0	value of a variable at $x = 0$
∞	value of a variable at infinity
w	value of a variable at the wall
x, y	partial derivative with respect to x, y

INTRODUCTION

The flow and heat transfer in the boundary layer induced by a continuous surface moving with uniform or non-uniform velocity in an ambient fluid are important in many manufacturing processes in industry such as the extrusion of a plastic sheet, the cooling of a metallic plate in a cooling bath and the boundary layer along material handling conveyers. Glass blowing, continuous casting and spinning of fibers also involve the flow due to a stretching surface. Sakiadis [1] was the first to study

* Correspondence and reprints.

the flow induced by a surface moving with a constant velocity in an ambient fluid. The corresponding heat transfer problem was studied theoretically by Tsou et al. [2], Erickson et al. [3] and experimentally by Griffin and Throne [4]. Crane [5] considered the same problem as studied in [1], but assumed that the surface velocity varies linearly with the stream-wise distance x ($U = ax$, $a > 0$). Since then several investigators [6–16] studied various aspects of this problem such as the heat transfer with uniform or non-uniform wall temperature or heat flux, mass transfer, suction or blowing, parallel free stream velocity, and a magnetic field. In all these cases self-similar solutions were obtained. The assumption of a linear variation of the wall velocity gives unrealistic wall velocity at $x = 0$. Jeng et al. [17] investigated the non-similar flow where the velocity of the stretching sheet was taken as $U = U_0(1 + x/L)$. The effect of the buoyancy force on the boundary layer flow over an inclined surface moving with a constant velocity in an ambient fluid was considered by Moutsoglou and Chen [18].

In this paper, we have studied the effect of the buoyancy force due to the thermal diffusion on the flow and heat transfer over a heated vertical or inclined surface moving with a non-uniform velocity, $U = U_0(1 + x/L)$, in an otherwise ambient fluid. Both constant wall temperature and constant heat flux conditions are included in the analysis. The coupled nonlinear partial differential equations are solved numerically using an implicit finite-difference scheme similar to that of Blottner [19]. The results are compared with those of Tsou et al. [2], Erickson et al. [3], Griffin and Throne [4], Jeng et al. [17] and Moutsoglou and Chen [18].

PROBLEM FORMULATION

We consider the laminar steady, incompressible boundary layer on a vertical or an inclined surface moving with a non-uniform velocity $U = U_0(1 + x/L)$ in an ambient fluid, where U is the wall velocity, U_0 is the value of the U at $x = 0$, L is the characteristic length and x is the distance measured from the leading edge (see *figure 1*). The buoyancy force acts vertically downwards. The wall temperature T_w and the ambient temperature T_∞ are both constant. The fluid properties are constant except the density variation required to drive the buoyancy forces. For the case of an inclined surface, both the stream-wise pressure gradient term and the buoyancy force term exist, but they have different magnitudes depending on the angle of inclination of the plate. The buoyancy induced stream-
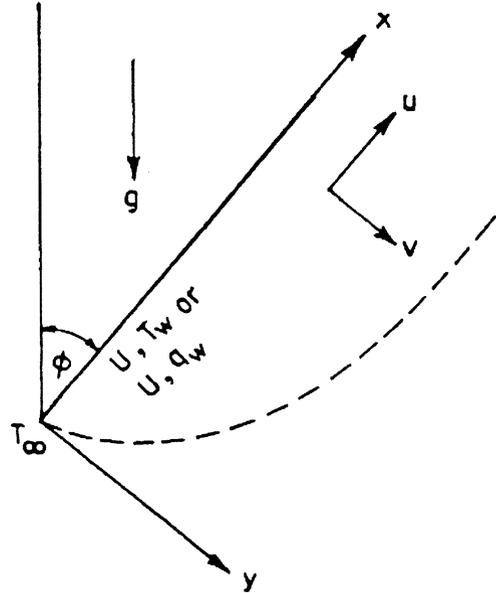

Figure 1. Schematic diagram of the physical system.

wise pressure gradient term can be neglected in comparison to the buoyancy force term if the condition $\tan \phi \ll Re_x^{1/2}/\eta_\infty$ is satisfied [20], where ϕ is the angle of inclination to the vertical, Re_x is the local Reynolds number and η_∞ is the edge of the boundary layer. For boundary layer flows, Re_x lies between 10^3 to 10^5. For $Re_x = 10^3$, $\eta_\infty = 10$, $\phi \leq 45°$ and $Re_x = 10^{5}, \eta_\infty = 10$, $\phi \leq 80°$. For a vertical plate $\phi = 0$. Under the above assumptions, the boundary layer equations governing the flow can be expressed as [12, 17, 18]

$$u_x + v_y = 0 \tag{1}$$

$$uu_x + vu_y = \nu u_{yy} + g\beta(T - T_\infty)\cos\phi \tag{2}$$

$$uT_x + vT_y = \alpha T_{yy} \tag{3}$$

The boundary conditions are given by

$$u(x, 0) = U(x), \qquad v(x, 0) = 0$$
$$T(x, 0) = T_w \quad \text{or} \quad T_y(x, 0) = -q_w/k$$
$$u(x, \infty) = 0, \qquad T(x, \infty) = T_\infty$$
$$u(0, y) = 0, \qquad T(0, y) = T_\infty, \quad y > 0. \tag{4}$$

Here x and y are the distances along and perpendicular to the surface; u and v are the velocity components along the x and y directions respectively; T is the temperature; g is the gravitational acceleration; β is the volumetric coefficient of thermal expansion; α is the thermal diffusivity; ν is the kinematic viscosity; q_w is the rate of heat transfer at the wall; k is the thermal conductivity;

the subscripts x and y denote derivatives with respect to x and y, respectively; and the subscripts w and ∞ denote conditions at the wall and in the ambient fluid, respectively.

In order to make the equations (1)–(3) dimensionless, we apply the following transformations

$$\eta = (2\overline{\xi}\nu)^{-1/2} U y$$

$$\overline{\xi} = \int_0^x U(x)\,\mathrm{d}x, \qquad \xi = x/L, \qquad U = U_0(1+\xi)$$

$$\Psi(x,y) = (2\nu\overline{\xi})^{1/2} f(\overline{\xi}, \eta)$$

$$\overline{\xi} = U_0 L \xi (1+\xi/2), \qquad u = \partial\Psi/\partial y = U f'(\overline{\xi},\eta)$$

$$v = -\partial\Psi/\partial x = -(2\overline{\xi}\nu)^{1/2}(U/2\overline{\xi})$$
$$\times \left[f + 2\overline{\xi}\,\partial f/\partial\overline{\xi} + (s_1-1)\eta f' \right]$$

$$\theta = (\overline{\xi},\eta) = (T - T_\infty)/(T_w - T_\infty)$$

$$\lambda = Gr_L/Re_L^2, \qquad Re_L = U_0 L/\nu$$

$$Gr_L = g\beta(T_w - T_\infty)L^3/\nu^2$$

$$Re_x = U_0 x/\nu, \qquad Pr = \nu/\alpha \qquad (5)$$

to equations (1)–(3) for the constant wall temperature case (CWT) case) we find that (1) is identically satisfied and (2) and (3) reduce to

$$f''' + ff'' - s_1 f'^2 + \lambda\cos\phi\, s_2\theta$$
$$= s_3\xi\left(f'\partial f'/\partial\xi - f''\partial f/\partial\xi\right) \qquad (6)$$
$$Pr^{-1}\theta'' + f\theta' = s_3\xi\left(f'\partial\theta/\partial\xi - \theta'\partial f/\partial\xi\right) \qquad (7)$$

where

$$s_1 = (2\overline{\xi}/U)\,\mathrm{d}U/\mathrm{d}\overline{\xi} = 2\xi(1+\xi/2)(1+\xi)^{-2}$$
$$s_2 = (2\overline{\xi}/U_0 L)/(U/U_0)^2 = 2\xi(1+\xi/2)(1+\xi)^{-3} \qquad (8)$$
$$s_3 = (2\overline{\xi}/UL) = 2(1+\xi/2)(1+\xi)^{-1}.$$

The boundary conditions for the CWT case are given by:

$$f(\xi,0) = 0, \qquad f'(\xi,0) = \theta(\xi,0) = 1$$
$$f'(\xi,0) = \theta(\xi,\infty) = 0. \qquad (9)$$

The corresponding equations for the constant heat flux case (CHF case) are given by:

$$f''' + ff'' - s_1 f'^2 + \lambda^*\cos\phi\, s_4\theta$$
$$= s_3\xi\left(f'\partial f'/\partial\xi - f''\partial f/\partial\xi\right) \qquad (10)$$
$$Pr^{-1}\theta'' + f\theta' - s_5 f'\theta = s_3\xi\left(f'\partial\theta/\partial\xi - \theta'\partial f/\partial\xi\right) \qquad (11)$$

where

$$T - T_\infty = (q_w/k)(2\overline{\xi}\nu)^{1/2} U^{-1}\theta(\overline{\xi},\eta)$$
$$\lambda^* = Gr_L^*/Re_L^{5/2}$$
$$Gr_L^* = g\beta q_w L^4(k\nu^2)$$
$$s_4 = (2\overline{\xi}/U_0 L)^{3/2}(U/U_0)^{-4} \qquad (12)$$
$$= \left[2\xi(1+\xi/2)^{3/2}(1+\xi)^{-4}\right]$$
$$s_5 = (U/U_0)^{-2} = (1+\xi)^{-2}.$$

The boundary conditions for the CHF case are given by

$$f(\xi,0) = 0, \qquad f'(\xi,0) = 1,$$
$$\theta'(\xi,0) = -1, \qquad f'(\xi,\infty) = \theta(\xi,\infty) = 0. \qquad (13)$$

Here $\overline{\xi}$ and η are the transformed coordinates; ξ is the dimensionless distance along the surface, ψ and f are the dimensional and dimensionless stream functions, respectively; θ is the dimensionless temperature; Gr_L and Gr_L^* are the Grashof numbers for the CWT and CHF cases, respectively; λ and λ^* are the buoyancy parameters for the CWT and CHF cases, respectively; Re_L is the Reynolds number; Pr is the Prandtl number; s_1, s_2, s_3, s_4 and s_5 are functions of ξ; and prime denotes derivative with respect to η.

It may be noted that for the CWT case equations (6) and (7) for $\lambda = 0$ (without buoyancy force) and $\xi = 0$ (self-similar flow) reduce t_0 those of Tsou et al. [2], Erickson et al. [3] and Griffin and Throne [4], if we apply the transformation.

$$\eta_1 = 2^{1/2}\eta, \qquad f_1(\eta_1) = 2^{1/2} f(\eta),$$
$$\theta_1(\eta_1) = \theta(\eta). \qquad (14)$$

Also for $\lambda = 0$, equations (6) and (7) for the CWT case reduce to those of Jeng et al. [17]. Further the $U = U_0$, equations (6) and (7) as well as (10) and (11) reduce to those of Moutsoglou and Chen [18] if we put $s_1 = 0$, $s_2 = s_4 = 2\xi$, $s_3 = 2$, $s_5 = 1$ and use the transformations (14).

The local skin friction coefficient C_{fx} is expressed as

$$C_{fx} = -2\mu(\partial u/\partial y)_{y=0}/\rho U^2$$
$$= -2^{1/2} Re_x^{-1/2}(1+\xi/2)^{-1/2} f''(\xi,0). \quad (15a)$$

The local Nusselt number Nu_x for the CWT case is given in the form

$$Nu_x = -x(\partial T/\partial y)_{y=0}/(T_w - T_\infty)$$
$$= -2^{1/2} Re_x^{1/2}(1+\xi)(1+\xi/2)^{-1/2}\theta'(\xi,0). \quad (15b)$$

Similarly, for the CHF case, the local Nusselt number is given by:

$$Nu_x = -2^{1/2}Re_x^{1/2}(1 + \xi/2)^{-1/2}(1 + \xi)/\theta(\xi, 0) \quad (15c)$$

where μ is the coefficient of dynamic viscosity.

NUMERICAL METHOD

The coupled nonlinear partial differential equations (6) and (7) under the boundary conditions (9) have been solved by using an implicit, iterative tri-diagonal finite-difference scheme similar to that of Blottner [19]. All the first-order derivatives with respect to ξ are replaced by two-point backward difference formulae of the form

$$(\partial R/\partial \xi)_{n,m+1} = (R_{n,m+1} - R_{n,m})/\Delta \xi \quad (16a)$$

$$R_{n,m} = R(\eta_n, \xi_m), \quad \eta_n = (n - 1)\Delta \eta, \\ n = 1, 2, \ldots, N \quad (16b)$$

$$\eta_\infty = \eta_N, \quad \xi_m = m\Delta \xi, \quad m = 0, 1, 2, \ldots$$

where R denotes the dependent variable f or θ and m and n the node locations along the ξ and η directions, respectively. First, the third-order equation (6) is converted to second-order equation by substituting $f' = F$. Then the second-order derivatives in η direction for F and θ are discretized using three-point central-difference formulae while the first-order derivatives are discretized by employing the trapezoidal rule. At each line of constant ξ, a system of algebraic equations is obtained. The nonlinear terms are evaluated at the previous iteration.

The system of linear algebraic equations can be written using matrix notation as

$$\vec{A}_n\vec{\omega}_{n-1} + \vec{B}_n\vec{\omega}_n + \vec{C}_n\vec{\omega}_{n+1} = \vec{D}_n, \quad n = 2, 3, \ldots, N - 1 \quad (17a)$$

where the vectors and the coefficient matrices are given by

$$\vec{\omega}_n = \begin{bmatrix} F \\ \theta \end{bmatrix}_{n,m+1}, \quad \vec{A}_n = \begin{bmatrix} A_{11} & 0 \\ 0 & A_{22} \end{bmatrix}_{n,m}$$

$$\vec{B}_n = \begin{bmatrix} B_{11} & B_{12} \\ 0 & B_{22} \end{bmatrix}_{n,m}, \quad \vec{C}_n = \begin{bmatrix} C_{11} & 0 \\ 0 & C_{22} \end{bmatrix}_{n,m}$$

$$\vec{D}_n^T = (D_1, D_2)_{n,m}, \quad \vec{\omega}_1^T = (1, 1), \quad \vec{\omega}_N^T = (0, 0). \quad (17b)$$

An algorithm that can be used to obtain the solution $\vec{\omega}_n$ at a certain stream-wise distance ξ, i.e., for a particular value of m is [21]

$$\vec{\omega}_n = -\vec{E}_n\vec{\omega}_{n+1} + \vec{J}_n, \quad 1 \le n \le N - 1 \quad (18a)$$

where

$$\begin{cases} \vec{E}_n = (\vec{B}_n - \vec{A}_n\vec{E}_{n-1})^{-1}\vec{C}_n \\ \vec{J}_n = (\vec{B}_n - \vec{A}_n\vec{E}_{n-1})^{-1}(\vec{D}_n - \vec{A}_n\vec{J}_{n-1}) \\ 2 \le n \le N - 1 \end{cases} \quad (18b)$$

and

$$\vec{E}_1 = \vec{E}_N = \begin{bmatrix} 0 & 0 \\ 0 & 0 \end{bmatrix}, \quad \vec{J}_1 = \begin{bmatrix} 1 \\ 1 \end{bmatrix}, \quad \vec{J}_N = \begin{bmatrix} 0 \\ 0 \end{bmatrix}. \quad (18c)$$

Knowing the values of the dependent variables and appropriate derivatives at m, corresponding to distance ξ, the dependent variables $\vec{\omega}_n$ at $m + 1$, which correspond to distance $\xi + \Delta \xi$ can be computed by using the following procedure. First, the values of the matrix elements A_{11}, B_{11} etc. are evaluated using the known values of the required variables at m. Next, with the help of (18b) and (18c), the $\vec{E}_n$ and $\vec{J}_n$ based on the values of the variables at m are calculated for all n between 1 and N, starting at the wall ($n = 1$) and values of $\vec{E}_n$ and $\vec{J}_n$ in (18a) and using the boundary conditions (18c), the values of the dependent variables $\vec{\omega}_n$ at $m + 1$ are determined in the reverse order, i.e., starting from $n = N$. New values of f at $m + 1$ are obtained from

$$f_{n,m+1} = \int_0^\eta F_{n,m+1} \, d\eta. \quad (19)$$

The process of improving $\vec{\omega}_n$ at $m + 1$ is repeated till the following convergence criterion is satisfied

$$\max\left[\left|\left(\frac{\partial F}{\partial \eta}\right)_{\eta=0}^{j+1} - \left(\frac{\partial F}{\partial \eta}\right)_{\eta=0}^{j}\right|, \\ \left|\left(\frac{\partial \theta}{\partial \eta}\right)_{\eta=0}^{j+1} - \left(\frac{\partial \theta}{\partial \eta}\right)_{\eta=0}^{j}\right|\right] < 10^{-4} \quad (20)$$

where the superscripts $j + 1$ and j denote the values for the current and previous iterations.

However, to start the solutions, the values of ω_n and f at $\xi = 0$ have to be calculated by solving the self-similar equations obtained by putting $\xi = 0$ in (6) and (7) under the boundary conditions (9) by a method analogous to that described above. To initiate the computation, initial profiles are chosen satisfying the boundary conditions (9) and these are given by

$$F = \theta = 1 - (\eta/\eta_\infty), \quad f = \eta - (\eta^2/2\eta_\infty). \quad (21)$$

In a similar manner, equations (10) and (11) under boundary conditions (13) corresponding to the CHF case are also solved.

RESULTS AND DISCUSSION

Equations (6) and (7) under the conditions (9) and equations (10) and (11) under the conditions (13) have been solved numerically using the method described in the previous section. In order to assess the accuracy of our method, we have compared the velocity profile u/U_0 for $\xi = \lambda = s_1 = 0$ with the theoretical and experimental results of Tsou et al. [2] in *figure 2*. The velocity profile is in very good agreement with the theoretical values. It also agrees well with the experimental values near the wall. Also we have compared the local Nusselt number Nu_x for $\xi = \lambda = s_1 = 0$ with the theoretical values of Erickson et al. [3] and with the experimental values of Griffin and Throne [4]. For direct comparison, we have to divide our results by $2^{1/2}$. The results are found to be in good agreement with the theoretical and experimental results when the wall velocity $U_0 \geq 8.92$ ft·sec^{-1}. The comparison is presented in *figure 3*. Further we have compared the surface shear stress, $f''(\xi, 0)$, and the surface heat transfer, $-\theta'(\xi, 0)$ values for $s_1 = 0$, $s_2 = s_4 = 2\xi$, $s_3 = 2$, $s_5 = 1$ with those of Moutsoglou and Chen [18]. For direct comparison we have to divide our results by $2^{1/2}$. The results are in excellent agreement. For the sake of brevity, the comparison is presented only for the case of constant wall temperature (CWT case) in *table I*.

The justification for dividing our results by $2^{1/2}$ is that our equations (6) and (7) are slightly different from those of [3, 4, 18] due to scaling effect. However, (6) and (7) could be reduced to their equations if we use the transformations given in equation (14). From (14) it is evident that the surface shear stress and heat transfer,
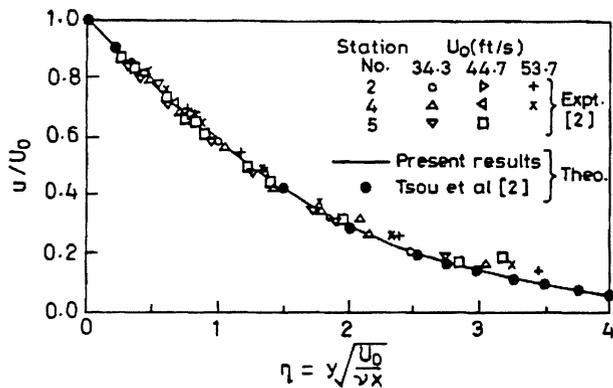
$\frac{\partial^2 f}{\partial \eta^2}(\xi, 0)$ and $-\frac{\partial \theta}{\partial \eta}(\xi, 0)$ are related to their results

$$\frac{\partial^2 f}{\partial \eta^2}(\xi, 0) = 2^{1/2}\frac{\partial^2 f_1}{\partial \eta_1^2}(\xi, 0)$$

$$\frac{\partial \theta}{\partial \eta}(\xi, 0) = 2^{1/2}\frac{\partial \theta_1}{\partial \eta_1}(\xi, 0). \tag{22}$$
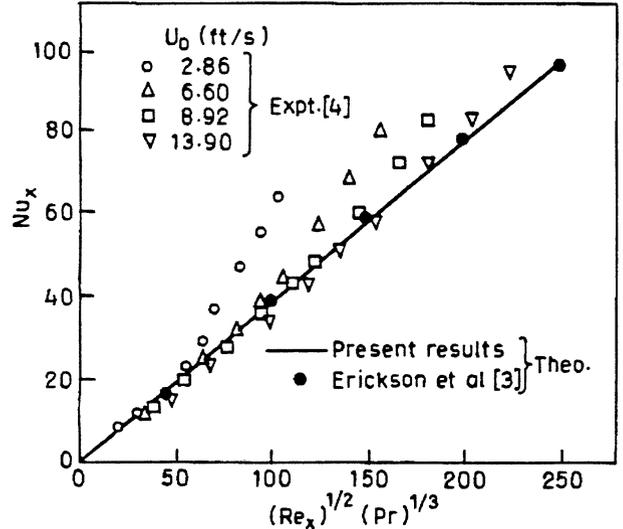

Figure 3. Comparison of the local Nusselt number, Nu_x, for $\xi = \lambda = s_1 = 0$ with that of Erickson et al. [3] and Griffin and Throne [4].

TABLE I
Comparison of the surface shear stress, $f''(\xi, 0)$ and the surface heat transfer $-\theta'(\xi, 0)$, for the CWT case when $s_1 = 0$, $s_2 = 2\xi$, $s_3 = 2$ with those of Moutsoglou and Chen [18].

		Present results		Moutsoglou and Chen [18]	
Pr	ξ	$f''(\xi, 0)$	$-\theta'(\xi, 0)$	$f''(\xi, 0)$	$-\theta'(\xi, 0)$
0.7	0	−0.44372	0.34922	−0.44375	0.34924
0.7	0.5	−0.10556	0.41317	−0.10558	0.41320
0.7	1.0	0.19423	0.45502	0.19425	0.45505
0.7	1.5	0.47217	0.47761	0.47214	0.47764
0.7	2.0	0.73556	0.50035	0.73552	0.50031
0.7	3.0	1.23107	0.53685	1.23103	0.53681
0.7	4.0	1.69657	0.56613	1.69652	0.56609
0.7	5.0	2.13993	0.59090	2.13988	0.59086
7.0	0	−0.44372	1.38698	−0.44375	1.38703
7.0	0.5	−0.28373	1.41317	−0.28376	1.41322
7.0	1.0	−0.12874	1.43706	−0.12876	1.43712
7.0	1.5	0.02107	1.45932	0.02105	1.45938
7.0	2.0	0.16883	1.48032	0.16880	1.48026
7.0	3.0	0.45321	1.53647	0.45318	1.53641
7.0	4.0	0.72694	1.55340	0.72697	1.55334
7.0	5.0	0.99207	1.58517	0.99201	1.58510

Figure 2. Comparison of the velocity profile u/U_0 for $\xi = \lambda = s_1 = 0$ with the theoretical and experimental results of the Tsou et al. [2].
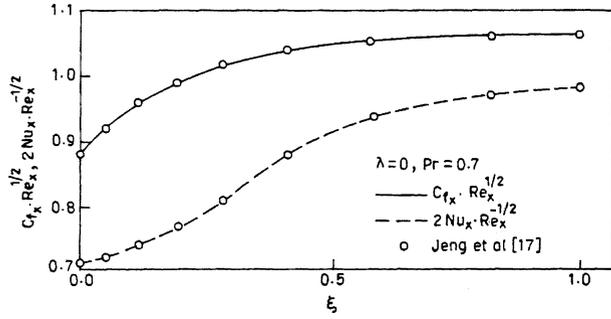
Figure 4. Comparison of the local skin friction coefficient, $Re_x^{1/2}C_{fx}$, and the local Nusselt number, $Re_x^{-1/2}Nu_x$ for $\lambda = 0$ with those of Jeng et al. [17].
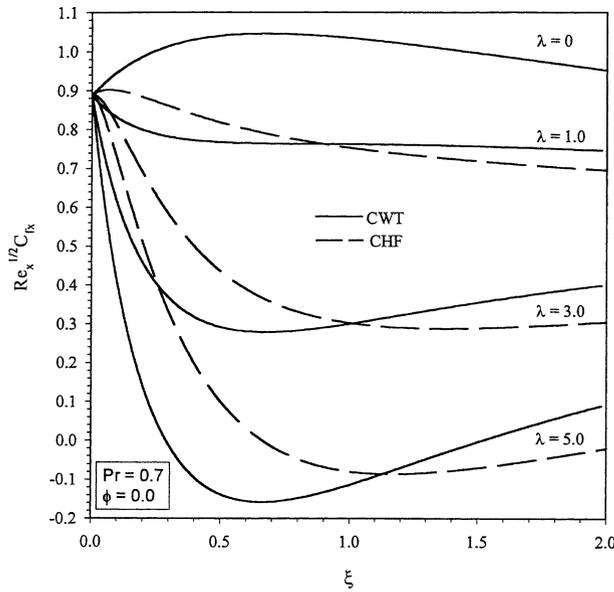

Figure 5. Effect of the buoyancy parameter, λ, on the local skin friction coefficient, $Re_x^{1/2}C_{fx}$, for the CWT and CHF cases.

Figure 6. Effect of the buoyancy parameter, λ, on the local Nusselt number, $Re_x^{-1/2}Nu_x$, for the CWT and CHF cases.

Also, for he CWT case, the skin friction coefficient, $Re_x^{1/2}C_{fx}$, and the Nusselt number, $2Re_x^{-1/2}Nu_x$, for $\lambda = 0$ are compared with those of Jeng et al. [17]. The results are found to be in very good agreement. The comparison is shown in *figure 4*.

For the CWT and CHF cases the effect of the buoyancy parameter, λ, on the local skin friction coefficient, $Re_x^{1/2}C_{fx}$, and the local Nusselt number, $Re_x^{-1/2}Nu_x$ for $0 \le \xi \le 2$, $Pr = 0.7$ is shown in *figures 5* and *6*, respectively. The skin friction coefficient strongly depends on the buoyancy parameter λ for $\xi > 0$, because λ explicitly occurs in the momentum equation (see equation (6)). The skin friction coefficient changes sign for $\lambda \ge 5$ at certain ξ locations. For $\lambda = 5$, $Pr = 0.7$, it changes sign at
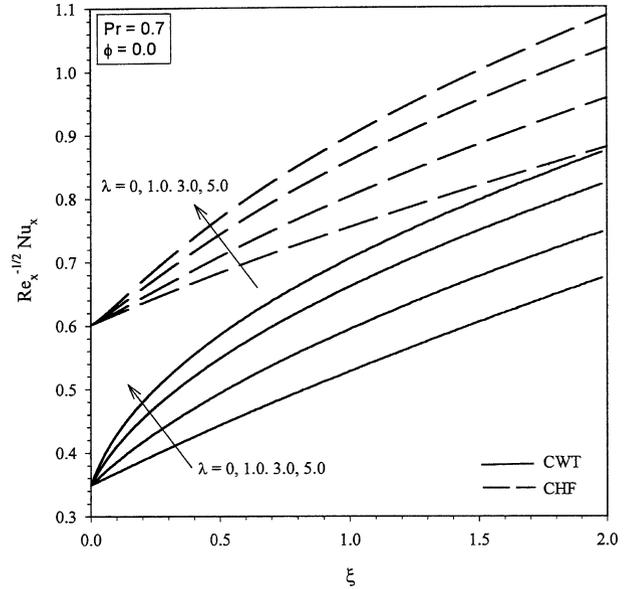
$\xi = 0.291$ and $\xi = 1.64$ for the CWT case and $\xi = 0.67$ and $\xi = 2.13$ for the CHF case. The vanishing of the skin friction at the surface does not imply separation since we are considering a moving wall problem [22]. The effect of λ on the skin friction coefficient and the Nusselt number for the CHF case is quantitatively similar to that of the CWT case. Hence, it is not discussed here. However, the Nusselt number for the CHF case is more than that of the CWT, but the skin friction coefficient for the CHF case is less or greater than that of the CWT case when $\xi < \xi_0$. For a surface moving in an ambient fluid, the gradient of the velocity on the surface $f''(\xi, 0) < 0$ and for $\lambda = 5$ it becomes positive in the range $0.291 < \xi < 1.64$ when $Pr = 0.7$. Similar trend has been observed by Moutosoglou and Chen [18] when the wall velocity is uniform. For $\xi = 2$, $Pr = 0.7$, the local skin friction coefficient changes (reduces) by about 9 times its value at $\lambda = 0$ as λ increases from zero to 5. The reason for this reduction with increasing λ is that the positive buoyancy parameter acts like a favorable pressure gradient which accelerates the fluid in the boundary layer. Consequently, the relative velocity between the wall and the fluid decreases as λ increases. The Nusselt number, $Re_x^{-1/2}Nu_x$, increases with the buoyancy parameter λ for $\xi > 0$ and the effect of λ becomes more pronounced with increasing ξ. The reason for this trend is that the buoyancy parameter ($\lambda > 0$) accelerates the fluid in the boundary layer (as mentioned earlier) which results in thinner thermal boundary layer. This in turn increases
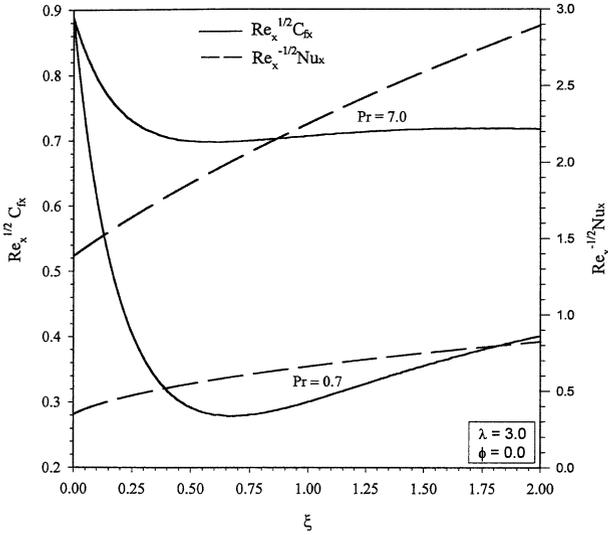
Figure 7. Effect of the Prandtl number, Pr, on the local skin friction coefficient, $Re_x^{1/2}C_{fx}$ and the local Nusselt number, $Re_x^{-1/2}Nu_x$ for the CWT case.

the Nusselt number as λ increases. Since λ is multiplied by $s_2(\xi) \geq 0$ (see equations (6) and (8)), there is no effect of λ at $\xi = 0$, since $s_2(\xi) = 0$ at $\xi = 0$, but it increases with ξ. For $\xi = 2$, $Pr = 0.7$, the Nusselt number increases by about 46% as λ increases from zero to 5. The reason for comparatively weaker dependence of the Nusselt number on λ is that the buoyancy parameter does not occur explicitly in the energy equation (see equation (7)).

Figure 7 presents the effect of the Prandtl number Pr on the skin friction ($Re_x^{1/2}C_{fx}$) and the Nusselt number ($Re_x^{-1/2}Nu_x$) for $\lambda = 3$, $0 \leq \xi \leq 2$ and for the CWT case. Since an increase in the Prandtl number reduces both the momentum and thermal boundary layers, the skin friction and the Nusselt number increase with Pr. For $\xi = 2$, $\lambda = 3$, the skin friction and the Nusselt number increase, respectively, by about 120% and 438% as Pr increases from 0.7 to 15.

The effect of the buoyancy parameter λ on the velocity and temperature profiles ($f'(\xi, \eta), \theta(\xi, \eta)$) for $\xi = 1$, $Pr = 0.7$ and for the CWT case is displayed in *figure 8*. As mentioned earlier, the positive buoyancy force acts like a favorable pressure gradient and hence accelerates the fluid in the boundary layer. This results in higher velocity as λ increases. For $\lambda = 5$, the velocity of the fluid near the wall is more than that on the wall. Since thermal boundary layer is also reduced with increasing λ, the temperature is lowered.

In *figure 9* the effect of the Prandtl number Pr on the velocity and temperature profiles ($f'(\xi, \eta), \theta(\xi, \eta)$)
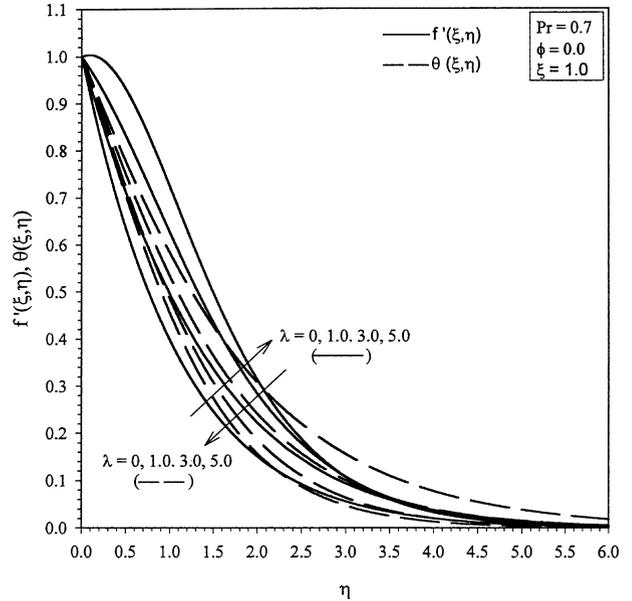

Figure 8. Effect of the buoyancy parameter, λ, on the velocity and temperature profiles, $f'(\xi, \eta)$ and $\theta(\xi, \eta)$, for the CWT case.
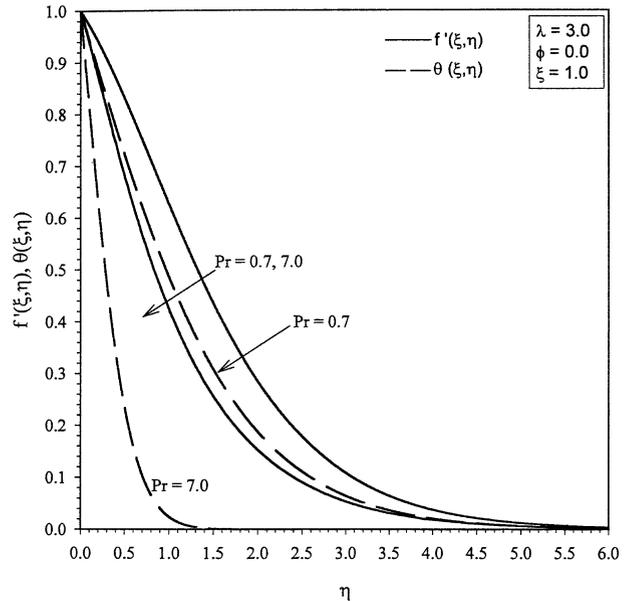

Figure 9. Effect of the Prandtl number, Pr, on the velocity and temperature profiles, $f'(\xi, \eta)$ and $\theta(\xi, \eta)$, for the CWT case.

for the CWT case when $\lambda = 3$, $\xi = 1$ is presented. Since the increase in the Prandtl number reduces both the momentum and thermal boundary layers, the velocity and temperature profiles decrease with increasing Pr. Also for large Pr the thermal boundary layer is much thinner
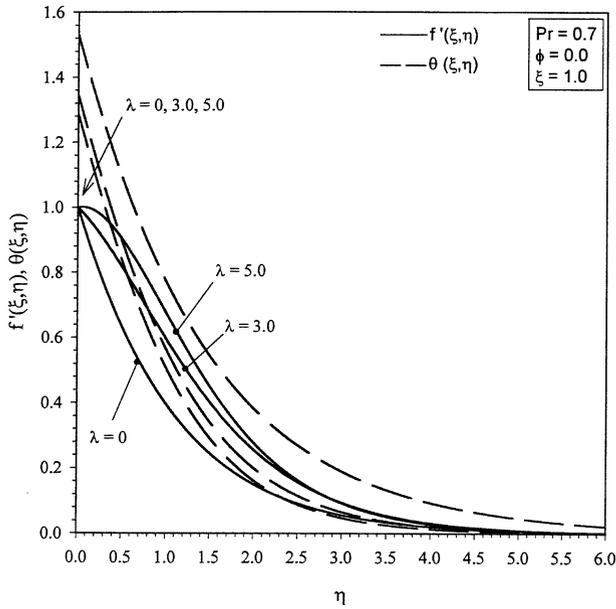
831

Figure 10. Effect of the buoyancy parameter, λ, on the velocity and temperature profiles, $f'(\xi, \eta)$ and $\theta(\xi, \eta)$, for the CHF case.
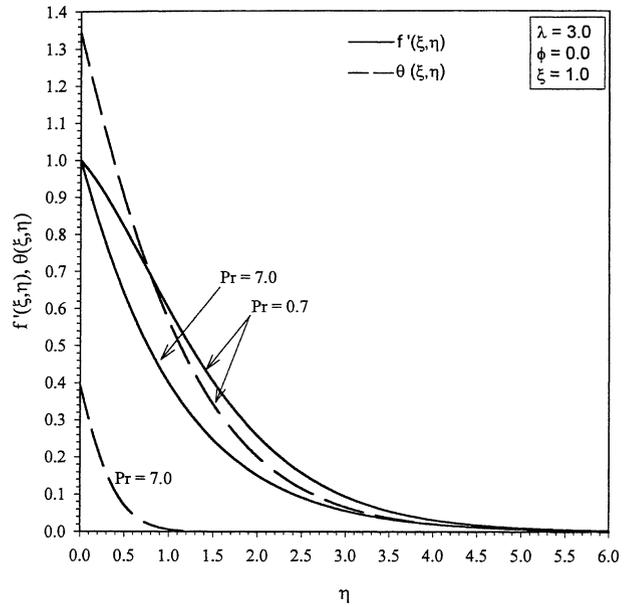

Figure 11. Effect of the Prandtl number, Pr, on the velocity and temperature profiles, $f'(\xi, \eta)$, $\theta(\xi, \eta)$, for the CHF case.

than the momentum boundary layer, because the effect of Pr is more pronounced on the temperature profiles than on the velocity profiles. This is due to the fact that Pr occurs explicitly in the energy equation.

For the CHF case, the effect of the buoyancy parameter λ on the velocity and temperature profiles ($f'(\xi, \eta)$, $\theta(\xi, \eta)$) for $Pr = 0.7$, $\xi = 1$ is displayed in *figure 10*. It is observed that the temperature at and near the wall is higher than that of the CWT case. Since the velocity profiles are qualitatively similar to those of the CWT case, the discussion is not presented here.

The effect of the Prandtl number Pr on the velocity and temperature profiles $f'(\xi, \eta), \theta(\xi, \eta)$, for the CHF case when $\lambda = 3$, $\xi = 1$ is shown in *figure 11*. The temperature at and near the wall changes very significantly unlike the CWT case where the change is small. The velocity profiles are qualitatively similar to those of the CWT case.

The effect of the inclination angle of the plate from the vertical, ϕ, on the skin friction and heat transfer, $Re_x^{1/2}C_{fx}$, $Re_x^{-1/2}Nu_x$ for $\lambda = 3$, $Pr = 0.7$ are presented in *figure 12*. For $\xi > 0$, the effect of ϕ is more pronounced on the skin friction coefficient than on the Nusselt number, because ϕ occurs explicitly in the momentum equation. The skin friction coefficient increases with ϕ, but the Nusselt number decreases.
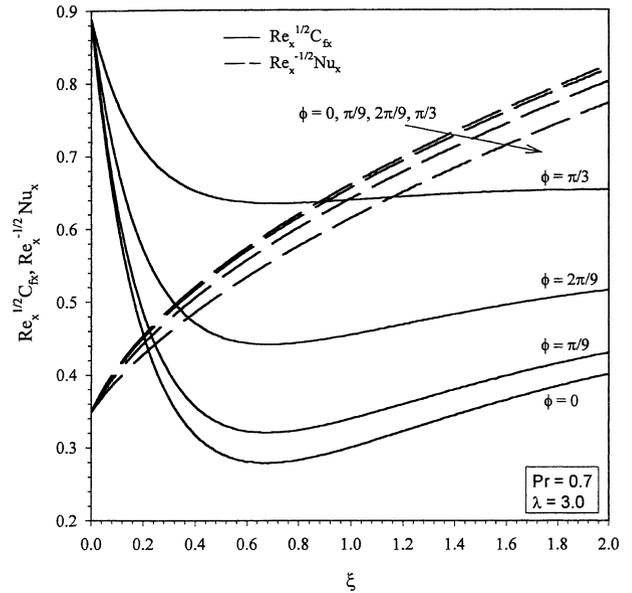

Figure 12. Effect of the inclination of the plate to the vertical, ϕ, on the local skin friction coefficient and Nusselt number, $Re_x^{1/2}C_{fx}$ and $Re_x^{-1/2}Nu_x$, for the CWT case.

CONCLUSIONS

It is evident from the results that the Nusselt number increases with the buoyancy force, the Prandtl number and the stream-wise distance. The skin friction increases

with the Prandtl number, but decreases with increasing buoyancy force. For buoyancy force greater than a certain value, the skin friction vanishes at certain locations downstream of the leading edge of the surface and it is positive in a certain range of stream-wise distance. However, it does not imply separation. Beyond a certain value of the buoyancy force the velocity of the fluid near the wall is more than that on the wall. The Nusselt number for the constant heat flux case is more than that of the constant wall temperature case. For large Prandtl number, the thermal boundary layer is much thinner than the momentum boundary layer.

REFERENCES

[1] Sakiadis B.C., Boundary layer behavior on continuous solid surface, II, The boundary layer on a continuous flat surface, AIChE. J. 7 (1961) 221–225.

[2] Tsou F.K., Sparrow E.M., Goldstein R.J., Flow and heat transfer in the boundary layer on a continuously moving surface, Internat. J. Heat Mass Transfer 10 (1967) 219–235.

[3] Erickson L.E., Fan L.T., Fox V.G., Heat and mass transfer on a moving continuous flat plate with suction or blowing, Ind. Engrg. Chem. Fund. 5 (1966) 19–25.

[4] Griffin J.F., Thorne J.L., On the thermal boundary layer growth on continuous moving belts, Amer. Inst. Chem. Engrg. J. 13 (1967) 1210–1211.

[5] Crane L.J., Flow past a stretching plate, ZAMP 21 (1970) 445–447.

[6] Gupta P.S., Gupta A.S., Heat and mass transfer on a stretching sheet with suction or blowing, Canad. J. Chem. Engrg. 55 (1977) 744–746.

[7] Chakrabarti A., Gupta A.S., Hydromagnetic flow, heat and mass transfer over a stretching sheet, Quart. Appl. Math. 33 (1979) 73–78.

[8] Carragher P., Crane L.J., Heat transfer on a continuously moving sheet, ZAMM 62 (1982) 564–565.

[9] Dutta B.K., Roy P., Gupta A.S., Temperature field in flow over a stretching sheet with uniform heat flux, Internat. Comm. Heat Mass Transfer 28 (1985) 1234–1237.

[10] Grubka L.J., Bobba K.M., Heat transfer characteristics of a continuous stretching surface with variable temperature, J. Heat Transfer 107 (1985) 248–256.

[11] Dutta B.K., Heat transfer from a stretching sheet with uniform suction or blowing, Acta Mech. 78 (1989) 255–262.

[12] Chappadi P.R., Gunnerson P.S., Analysis of heat and momentum transport along a moving surface, Internat. J. Heat Mass Transfer 32 (1989) 1383–1386.

[13] Anderson H.J., An exact solution of the Navier–Stokes equations for MHD flow, Acta Mech. 113 (1995) 241–244.

[14] Chiam T.C., Heat transfer with variable conductivity in a stagnation-point flow towards a stretching sheet, Internat. Comm. Heat Mass Transfer 23 (1996) 239–248.

[15] Vajravelu K., Hadjinicolaou A., Convective heat transfer in an electrically conducting fluid at a stretching surface in uniform free stream, Internat. J. Engrg. Sci. 35 (1997) 1237–1244.

[16] Kumari M., Nath G., Flow and heat transfer in a stagnation-point flow over a stretching sheet with a magnetic field, Mech. Res. Comm. 26 (1999) 469–478.

[17] Jeng D.R., Chang T.C.A., De Witt K.J., Momentum and heat transfer on a continuous moving surface, J. Heat Transfer 108 (1986) 532–539.

[18] Moutsoglou A., Chen T.S., Buoyancy effects in boundary layers on inclined continuous moving sheets, J. Heat Transfer 102 (1980) 71–178.

[19] Blottner F.G., Finite-difference method of solution of boundary layer equations, AIAA. J. 8 (1970) 193–205.

[20] Moutsoglou A., Chen T.S., Mixed convection on inclined surfaces, J. Heat Transfer 101 (1979) 422–426.

[21] Varga R.S., Matrix Iterative Analysis, Prentice-Hall, New York, 1962, p. 194.

[22] Williams J.C., Incompressible boundary-layer separation, Ann. Rev. Fluid Mech. 9 (1977) 113–144.